Hindawi Publishing Corporation
International Journal of Photoenergy
Volume 2013, Article ID 954914, 7 pages
http://dx.doi.org/10.1155/2013/954914

Research Article

Bactericidal Activity of TiO_2 on Cells of *Pseudomonas aeruginosa* ATCC 27853

J. L. Aguilar Salinas,[1] J. R. Pacheco Aguilar,[2] S. A. Mayén Hernández,[2] and J. Santos Cruz[2]

[1] *Facultad de Ingeniería, Universidad Autónoma de Querétaro, 76010 QRO, Mexico*
[2] *Facultad de Química, Materiales, Universidad Autónoma de Querétaro, 76010 QRO, Mexico*

Correspondence should be addressed to J. Santos Cruz; jsantos@uaq.edu.mx

Received 25 May 2013; Revised 21 July 2013; Accepted 21 July 2013

Academic Editor: Guisheng Li

The photocatalytic activity of semiconductors is increasingly being used to disinfect water, air, soils, and surfaces. Titanium dioxide (TiO_2) is widely used as a photocatalyst in thin films, powder, and in mixtures with other semiconductors or metals. This work presents the antibacterial effects of TiO_2 and light exposure (at 365 nm) on *Pseudomonas aeruginosa* ATCC 27853. TiO_2 powder was prepared from a mixture of titanium isopropoxide, ethanol, and nitric acid using a green and short time sol-gel technique. The obtained gel annealed at 450°C was characterized by X-ray diffraction, Raman spectroscopy, ultraviolet-visible spectroscopy, diffuse reflectance, scanning electron microscopy, and transmission electron microscopy. The nanocomposite effectively catalyzed the inactivation of *Pseudomonas aeruginosa*. Following 90 minutes exposure to TiO_2 and UV light, logarithm of cell density was reduced from 6 to 3. These results were confirmed by a factorial design incorporating two experimental replicates and two independent factors.

1. Introduction

The gram-negative bacterium *Pseudomonas aeruginosa* (PA) is considered an opportunistic pathogen because it requires minimal nutrients to survive, can tolerate a wide variety of physicochemical conditions, and possesses one of the largest and most complex known prokaryotic genomes (conferring strong resistance to antibiotics). In addition, a high proportion of its proteins is involved in regulation, virulence functions, and transport. PA is a major cause of nosocomial infections, cystic fibrosis, ulcer-like keratitis, lung infections, and fatal diseases in immunocompromised individuals. Self-produced antibiotic-inactivating enzymes cause high antibiotic resistance, low outer membrane permeability, and the expression of genes encoding various efflux pumps [1–3]. One area of continuing study is the type of surfaces likely to harbor pathogens, as reservoirs of contamination present a significant health hazard. Common sources of infection are hospitals, food, both consumption and production centers, and public places.

In 1972, Fujishima and Honda demonstrated that titanium dioxide TiO_2 (TD) exhibits strong bactericidal activity in the presence of light ($\lambda \leq 385$ nm) [4]. To date, there have been several reports which tested the antibacterial activity of both powder in solution and surfaces coated with TD on clinically relevant microorganisms such as *Escherichia coli*, *Staphylococcus aureus*, *Listeria monocytogenes,* and *Pseudomonas aeruginosa* [5, 6].

At the cellular level, some researchers have found different modes of action of bactericidal activity on TD, between which there are two commonly accepted mechanisms that have been proposed for the bactericidal action of TD (i) direct oxidation of intracellular coenzyme A, leading to respiratory inhibition [7], and (ii) loss of potassium ions and the slow release of pathogenic proteins and RNA, resulting in death by intracellular disorder and cell wall decomposition [8]. Conversely, photocatalysis has been shown to promote destruction of the cell membrane [9]. Some studies have identified the most resistant pathogens as those with both complex gene expression systems and thickened cell walls [9–11]. The bactericidal activity of PA has been reported. Others researchers have found variable results, 100% inhibition in 25 minutes using TD solutions (1 mg/mL) [6] until reports

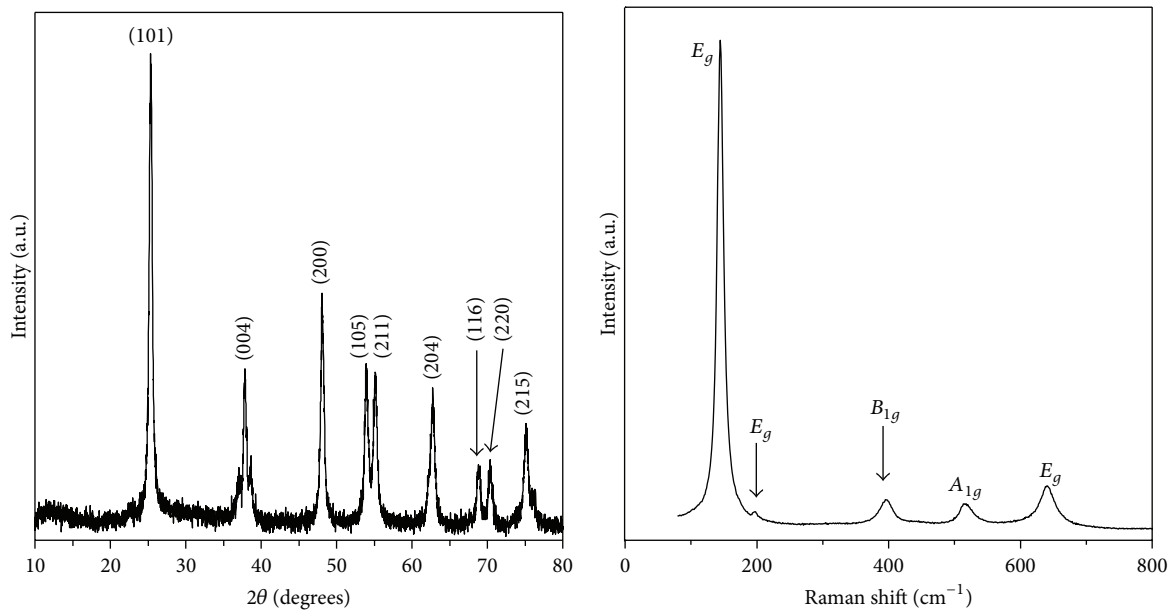

FIGURE 1: (a) Powder XRD of TiO_2 synthesized by sol-gel at 450°C. (b) Raman spectrum of TiO_2 powder obtained at 450°C.

indicate that the use of concentrations of 10 mg/mL of Ag doped TD with similar inhibition values reached in 120 minutes [12] and tests on films of TD. The nature of the materials used due to the synthesis and thermal treatment are some of the factors that have an influence on the antibacterial ability. Our group has obtained the synthesis of TD in thin film by the sol-gel method, according to the method reported in [13], obtaining good results in the degradation of methylene blue; however, antimicrobial activity was unknown in TD powder. So in this research paper we carried out the characterization and evaluated the antimicrobial effect of the TD powder on *Pseudomonas aeruginosa* ATCC 27853.

2. Experimental Methods

2.1. Powder of Titanium Dioxide. The titanium dioxide TiO_2 powder was prepared by the sol-gel technique from a precursor solution containing titanium isopropoxide, ethanol, deionized water, and nitric acid (molar ratio 2 : 72 : 6 : 1 [13]). The preparation of this solution requires an inert atmosphere. The precursor solution, thus prepared, was removed from the inert atmosphere and dried at 80°C until all solvents had evaporated. The powder obtained was annealed at 100°C for 1 hour and 450°C for another hour in an open atmosphere, after which, pure titanium dioxide powder was obtained. The characterization of the TD powders was carried out by XRD patterns and was registered using a Rigaku Miniflex$^+$ Diffractometer (CuKα_1 radiation, 1.54 Å). For the Raman measurements a Dilor Labram II microRaman was employed. The diffuse reflectance of the samples was measured using an Ocean Optic Spectrometer. The SEM and TEM images were obtained by a JEOL JSM-6060LV and JEOL JEM1010 microscopies, respectively.

2.2. Bactericidal Activity. Pseudomonas aeruginosa ATCC 27853 was grown in a 30 mL nutrient broth at 37°C for 16 h. The bacterial suspension was then centrifuged at 3,000 rpm for 10 min. and washed twice with saline solution (NaCl 0.85%). The resulting cell pellet was resuspended in 1 mL of saline solution, and cell density was determined using a Neubauer counting chamber. Prior to testing the antimicrobial properties of TiO_2, the cell count was adjusted to 10^6 cells mL^{-1}. The test itself was performed in glass vessels in which 10^6 cells were mixed with 0.5 and 1 mg (final volume 1 mL). A vessel without TiO_2 was prepared as a control.

The mixed solutions were irradiated with UVA (365 nm) from a black-light bulb (9 W). Exposure times were 30, 60, 90, and 120 min. Following exposure, the solution was sampled to determine the cell viable counts using the most probable number method (MPN). Decimal dilutions of samples were inoculated in quintuplicate in tubes containing nutrient broth and incubated at 37°C for 24 h. Tubes in which the solution had become turbid during incubation were considered positive for bacterial growth. Data from these tubes were used to calculate cell numbers and cell viability (as a percentage of all cells). The Degussa P25 (P25) was used in order to compare the TD synthesized for our experimental method. The characteristics of the P25 are nanopowder with 21 nm particle size (TEM), >99.5%.

3. Results and Discussion

X-ray diffraction (XRD) was performed on the TD powders to determine their phase and crystallinity. Figure 1(a) shows the XRD patterns with peaks at 2θ = 25.32, 37.82, 48.12, 53.94, 55.11, 62.76, 68.8, 70.38, and 75.14°, corresponding to the planes (101), (004), (200), (105), (211), (204), (116), (220), and (215), respectively. These planes closely match

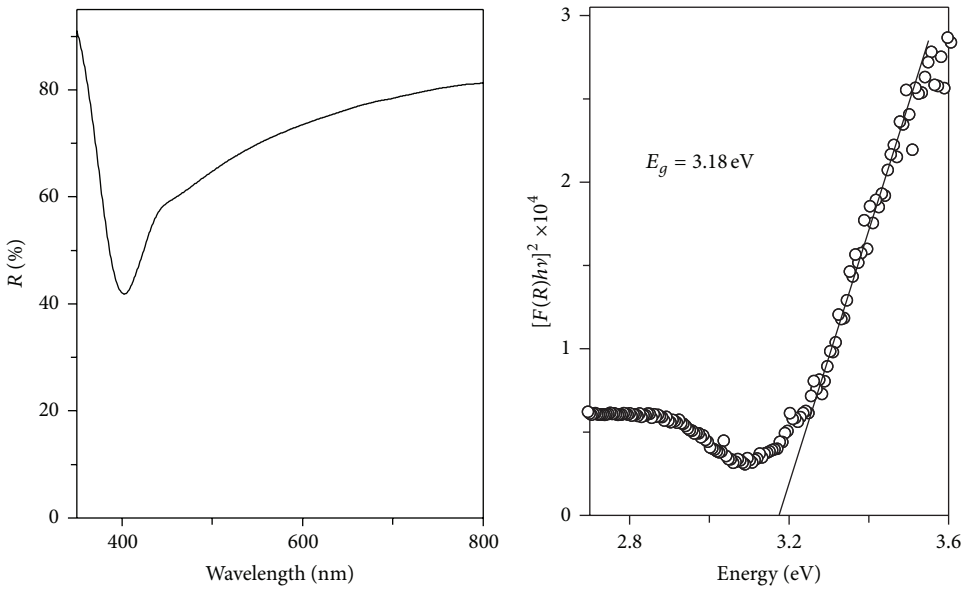

FIGURE 2: (a) Uv-Vis diffuse reflectance spectra of TiO_2 obtained at 450°C. (b) Band gap of the TiO_2 computed by Kubelka-Munk function, where E_g is the band gap energy, R is the reflectance of the TD, h is Planck's constants, and ν is the frequency of the radiation.

those of PDF number 78-2486, corresponding to the pure tetragonal anatase TD phase. The grain size, calculated from the XRD pattern using the Scherer formula, is 25.27±0.11 nm. The anatase phase in TD is one of the most important metal oxides in terms of potential applications to photonic crystals, sensors, smart surfaces coatings, photovoltaic cells, photocatalysis, and bactericidal agents and as such has been extensively studied [9, 14–17]. The phase of bactericidal TD powder was determined by Raman spectroscopy. The TD displays six Raman active modes of anatase phase, with symmetries of 3 vibrating modes for E_g, and 2 for B_{1g} and A_{1g}, corresponding to 144, 197, 399, 515, 519, and 639 cm^{-1} [18–20]. Figure 1(b) displays the Raman spectra of TD obtained at 450°C in an open atmosphere, in which the vibrating modes occur at 144, 196, 396, 516, and 638 cm^{-1}, consistent with those reported previously for the anatase phase [18–20].

Figure 2 shows the Uv-Vis diffuse reflectance spectra of TD powder annealed in an open atmosphere at 450°C. The maximum of the reflection edge can be estimated as 390 nm. From the plot of the Kubelka-Munk function versus the energy of the incoming radiation and supposing that the anatase phase of TD is an indirect band gap semiconductor, a band gap of 3.18 eV was obtained (Figure 2(b)).

The superficial structure of the TD annealing at 450°C was characterized by scanning electron microscopy (SEM) imaging (Figures 3(a) and 3(b)). The sample contains a range of particle sizes (diameter 30 to 1 micron). The larger particles comprise aggregates of smaller particles. Under transmission electron microscopy (TEM), the nanocrystalline form of the TD powder is revealed (Figures 3(c) to 3(e)). The TEM images display tetragonal nanocrystals with facets (001) and (101) of anatase phase. The space group is I4(1)/amd. Recently, it has been revealed that the reactivity of TD depends not only on its superficial separation properties but also on low recombination of bulk charge carriers and/or the ability of TD to tune its reaction preferences during reaction [21, 22]. Conversely, materials with structures such as (001) facets of anatase exhibited enhanced photocatalytic activity, because they efficiently generate $OH^{\bullet}$ radicals that promote the chemical destruction. In the context of our study, such radicals can penetrate the bacterial cell wall, leading to death of the bacterium.

The predominance of the facet is {001}, {101}, and {010} [23–25]. Figures 3(d) and 3(e) show the different morphologies obtained in the anatase TD nanocrystals. Similar results of the TEM images were found by Hao et al. [22] and Jiao et al. [24]. To control the crystal morphology, the exposed (001) and (101) facets (see insets) were synthesized via a green and short time sol-gel method in the absence of fluorine compounds, which are hazardous to both environment and health. Being the most electronegative element in the periodic table, fluorine is extremely reactive (corrosive and poisonous) and requires care in handling.

Figure 4 displays photocatalytic activity of the TD and commercial P25 (exposed to light at 365 nm) versus time, for concentrations 0.5 mg mL^{-1} (Figure 4(a)) and 1 mg mL^{-1} (Figure 4(b)). The black squares in both plots represent the effect of the light source only (control without TD and P25).

As revealed in Figure 4(a) the viability of cells exposed to 0.5 mg mL^{-1} TD was affected significantly at 60, 90, and 120 minutes after which 99, 99.92, and 100% and for P25 99.38, 99.996, and 100% of the microorganism, respectively, were killed. Similar results were obtained at 1 mg mL^{-1}, where cell viability was reduced by 99.7, 99.99, and 100% after 60, 90, and 120 min exposure, respectively, and the P25 99.997 and 100% for 60 and 90 min. With commercial P25 exposure

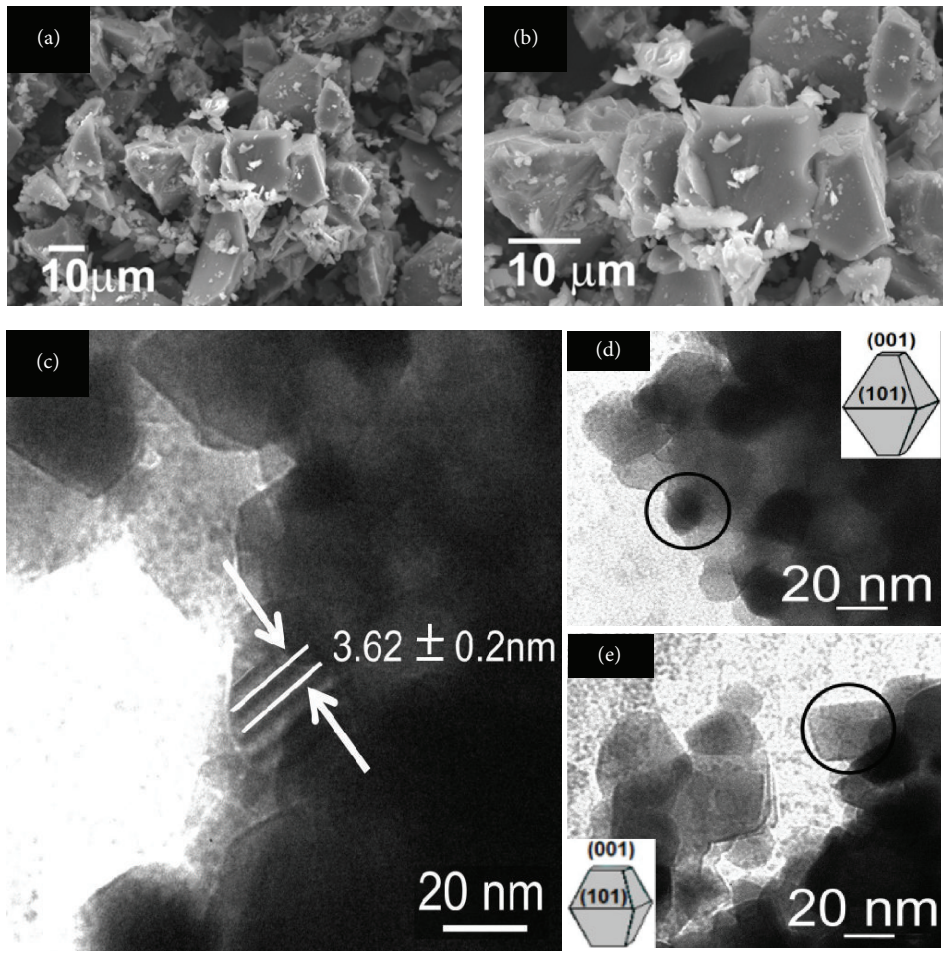

FIGURE 3: SEM and TEM images of the TiO_2 powder, magnified by (a) 1000x and (b) 2000x. (c) Morphology of the anatase (distance between marks is 3.8 nm). (d) 2D tetragons showing highly absorbing (001) facets and (e) images of TD synthetized in the absence of fluorine compounds. Insets of Figures (d) and (e) are representative sketches of the faceted nanoparticles.

to the same times, we can observe better results with 1% (times $\geq$ 60 minutes), see Figures 4(a) and 4(b). As a control, a solution with 1.7×10^6 and 9×10^5 cells mL^{-1} for 0.5 and 1 mg mL^{-1}, respectively, was utilized. They were exposed to UV light (365 nm), showing no change in the density population; this was maintained in the order of 10^6, so it discarded any inhibitory effect of UV light. The main difference between our TD and P25 is the crystal size. Currently in our laboratory, is underway additional work in order to find a new synthesis to obtain crystal size of the order of 21 nm, we probably get comparable results (closer) since it is well known that nanoparticles significantly increase the surface area. Ibáñez et al., 2003 [26], using Degussa P25 in a concentration of 0.1 mg mL^{-1} on PA ATCC, starting with a cell density of 10^6 to 10^7, after 40 min it observed that there is a decrease of 3 log. This is very comparable to the present study. Amézaga et al. 2003 [27] conducted a similar test on TiO_2 thin films (anatase phase) prepared on glass slides by the sol-gel process, in which it was found that *Pseudomonas aeruginosa* ATTC 27853 was inhibited by 32 to 72%, over a range of irradiation times (40 to 120 min). Under TEM they observed abnormal cell division after 40 min exposure to TiO_2/UV. At 240 min, wavy structures and bubble-like protuberances appeared, and intracellular material was expelled [22]. Some biochemical mechanisms have been proposed for the powerful bactericidal action of photocatalytic anatase TD powder in the presence of an illumination source. Illumination encourages the generation of highly reactive chemical oxidative species ($OH^{\bullet}$) that promote the peroxidation of phospholipid components in the lipid membrane and the oxidation of intracellular coenzymes, resulting in the inhibition of respiratory activity and subsequent cell death [7, 8, 26]. The intensity of the radiation used during the tests could have an effect on microbial inhibition. Robertson et al., 2005 [28], using Degussa P25 material at a concentration of 1 mg mL^{-1}, obtained a 3 log reduction of PA in a time of 2 h, which is comparable to the test performed in this study; however, it was found that they used a 480 W lamp with a 330 to 450 nm wavelength range, which had a bactericidal activity confirmed in the controls when the test was performed in the absence of Degussa P25, obtained for exposing the cells to UV light; higher percentages of inhibition were reached. In the present research work no inhibition was observed by UV light lamp in the controls.

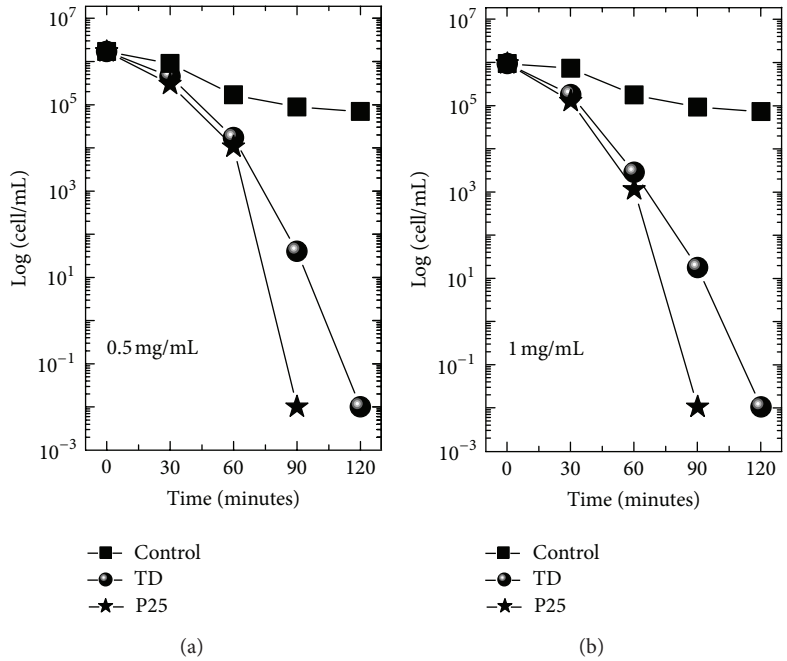

Figure 4: Effect of light and TiO_2 concentration on viability of the *Pseudomonas aeruginosa* ATCC 27853 exposed to (a) 0.5 mg mL^{-1} TD and P25 and (b) 1 mg mL^{-1} TD and P25. In both plots, the control data (light exposure without TD and P25) are displayed as black squares.

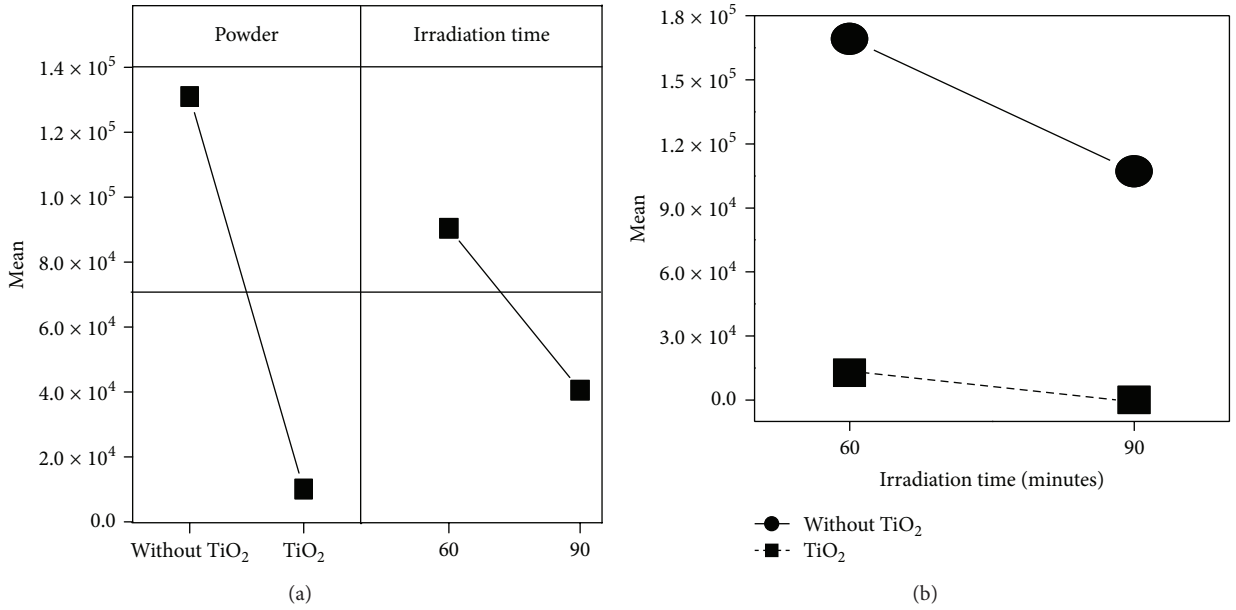

Figure 5: Principal effects and interaction between light and TD on the *Pseudomonas aeruginosa* survival at TD concentration 0.5 mg mL^{-1}.

The grain size could also be related to bactericidal activity due to the increase in the reaction surface. Ubonchonlakate et al. conducted a test in 2012 [29] with porous film with grain size of 15 to 25 nm, and they obtained close to 100% at 60 minutes for a cell density of PA 1×10^3 cells/mL. They also found that the use of porous materials and Ag particles reached almost 100% inhibition for 45 and 10 min, respectively. Similar results were obtained by Hitkova et al. 2012 [6] with thin films of TD, and they found efficiencies of 100% inhibition (10^5 cells/mL) in a 25 min. The particle size employed was 20 nm, the preparation time of the material was 340 h, and the thermal treatment was 500°C. In addition to particle size, the presence of Ag could influence the rapid reduction of cell viability, since it has been reported that this metal has bactericidal activity.

To assess the bactericidal effect of the anatase TD on *Pseudomonas aeruginosa*, the results were input to the Minitab program as an experimental design with two factors and two levels (results were analyzed at 60 and 90 minutes only). The computation was performed using full factorial design

Table 1: Experimental data entered for the experimental design run.

StdOrder	RunOrder	CenterPt	Blocks	Powder	t/min	Y_1 (0.5 mg/mL)	Y_2 (1 mg/mL)
5	1	1	1	WTD	60	1.690×10^5	1.69×10^5
4	2	1	1	TD	90	4.700×10^1	1.30×10^1
1	3	1	1	WTD	60	1.690×10^5	1.69×10^5
7	4	1	1	WTD	90	6.915×10^4	6.91×10^4
2	5	1	1	TD	60	1.275×10^4	2.16×10^3
6	6	1	1	TD	60	2.159×10^4	3.28×10^3
3	7	1	1	WTD	90	1.070×10^5	1.07×10^5
8	8	1	1	TD	90	3.300×10^1	2.10×10^1

Table 2: ANOVA factorial fit: Y_1 (0.5 mg mL^{-1}) versus TD powder and irradiation time.

Estimated effects and coefficients for Y_1 (0.5 mg/mL) (coded units)					
Term	Effect	Coeff	SE Coeff	T	P
Constant		68581	4861	14.11	**0.000**
TD	−119951	−59976	4861	−12.34	**0.000**
Irradiation time	−9037	−24518	4861	−5.04	**0.007**
TD × Irrad time	31906	15953	4861	3.28	**0.030**
S = 13750.1		PRESS = 3025065282			
R^2 = 97.92%		R^2 = 91.68%		**R^2 (adj) = 96.36%**	

with TD and WTD as the two factors and two replicates (see Table 1, where WTD is without TiO_2). To analyze the significance of factors, TD concentrations of 0.5 mg mL^{-1} and 1 mg mL^{-1} were considered separately, for two separate observations of the cell viability (Y_1 and Y_2), representing independent experiments.

The results of the factorial fit for 0.5 mg mL^{-1} powdered TD are presented in Table 2. We observe that the selected factors are significant at the 95% confidence level, because all of the P values are less than 0.05. The presence of TD powder, the exposure time, and the interaction between these two variables are similarly significant. The model further shows that the factorial design can account for 96.36% of the data behavior, confirming the bactericidal activity of the TD. At 1 mg mL^{-1} TD (data not shown) similar P values are obtained and the model fits 96.86% of the data.

Figure 5 presents the principal effects of light irradiation (at 365 nm), TD presence, and irradiation time, as well as their combined effects, on *Pseudomonas aeruginosa*. The presence of TD and exposure to light independently decrease the estimated bacterial population significantly. The interaction between exposure time and the presence of TD powder is also significant, and their combined impact is greater than that of either factor alone.

4. Conclusions

Powdered titanium dioxide in anatase phase with possible facets (001) and (010) was synthesized by the sol-gel technique from a simple, green, and short time route. The bactericidal properties of the synthesized compound were confirmed in aqueous solution. Titanium dioxide combined with illumination (at 365 nm) exerted significant antibactericidal activity. The efficacy of this activity was confirmed by factorial design, which demonstrated that the mortality of *Pseudomonas aeruginosa* ATCC 27853 exposed for 90 minutes to 0.5 and 1 mg mL^{-1} TD was 99.92 and 99.99%, respectively. The results consolidate previous reports of the unique physical and chemical properties of synthesized TiO_2 powder (namely, strong oxidizing and photocatalytic activity) that render it an effective bactericidal material.

Acknowledgment

Authors are grateful for technical assistance provided by IBQ Ma. Lourdes Palma Tirado, Neurobiology Institute of UNAM Juriquilla Qro., on the TEM measurements.

References

[1] R. E. W. Hancock, "Resistance mechanisms in *Pseudomonas aeruginosa* and other nonfermentative gram-negative bacteria," *Clinical Infectious Diseases*, vol. 27, no. 1, pp. S93–S99, 1998.

[2] N. Mesaros, P. Nordmann, P. Plésiat et al., "*Pseudomonas aeruginosa*: resistance and therapeutic options at the turn of the new millennium," *Clinical Microbiology and Infection*, vol. 13, no. 6, pp. 560–578, 2007.

[3] R. Vaisvila, R. D. Morgan, J. Posfai, and E. A. Raleigh, "Discovery and distribution of super-integrons among pseudomonads," *Molecular Microbiology*, vol. 42, no. 3, pp. 587–601, 2001.

[4] A. Fujishima and K. Honda, "Electrochemical photolysis of water at a semiconductor electrode," *Nature*, vol. 238, no. 5358, pp. 37–38, 1972.

[5] N. G. Chorianopoulos, D. S. Tsoukleris, E. Z. Panagou, P. Falaras, and G.-J. E. Nychas, "Use of titanium dioxide (TiO_2) photocatalysts as alternative means for *Listeria monocytogenes*

biofilm disinfection in food processing," *Food Microbiology*, vol. 28, no. 1, pp. 164–170, 2011.

[6] H. Hitkova, A. Stoyanova, N. Ivanova et al., "Study of antibacterial activity of nonhydrolytic synthesized TiO_2 againts *E. Collo*, *P. Aeruginosa* and *S. Aureus*," *Journal of Optoelectronics and Biomedical Materials*, vol. 4, no. 1, pp. 9–17, 2012.

[7] T. Matsunaga, R. Tomoda, T. Nakajima, and H. Wake, "Photoelectrochemical sterilization of microbial cells by semiconductor powders," *FEMS Microbiology Letters*, vol. 29, no. 1-2, pp. 211–214, 1985.

[8] T. Saito, T. Iwase, J. Horie, and T. Morioka, "Mode of photocatalytic bactericidal action of powdered semiconductor TiO_2 on mutans streptococci," *Journal of Photochemistry and Photobiology B*, vol. 14, no. 4, pp. 369–379, 1992.

[9] P. K. J. Robertson, J. M. C. Robertson, and D. W. Bahnemann, "Removal of microorganisms and their chemical metabolites from water using semiconductor photocatalysis," *Journal of Hazardous Materials*, vol. 211-212, pp. 161–171, 2012.

[10] N. Lydakis-Simantiris, D. Riga, E. Katsivela, D. Mantzavinos, and N. P. Xekoukoulotakis, "Disinfection of spring water and secondary treated municipal wastewater by TiO_2 photocatalysis," *Desalination*, vol. 250, no. 1, pp. 351–355, 2010.

[11] S. Malato, P. Fernández-Ibáñez, M. I. Maldonado, J. Blanco, and W. Gernjak, "Decontamination and disinfection of water by solar photocatalysis: recent overview and trends," *Catalysis Today*, vol. 147, no. 1, pp. 1–59, 2009.

[12] S. Khan, I. A. Qazi, Hasmi, M. A. Awan, and N. S. Zaidi, "Synthesis of silver-doped titanium TiO_2 powder-coated surfaces and its ability to inactive *Pseudomona aeruginosa* and bacillus subtilis," *Journal of Nanomaterials*, vol. 2013, Article ID 531010, 8 pages, 2013.

[13] J. G. Mendoza-Alvarez, A. Cruz-Orea, O. Zelaya-Angel et al., "Characterization of TiO_2 thin films for photocatalysis applications using photoacoustic spectroscopy," *Journal De Physique IV France*, vol. 125, pp. 407–409, 2005.

[14] X. Chen and S. S. Mao, "Titanium dioxide nanomaterials: synthesis, properties, modifications and applications," *Chemical Reviews*, vol. 107, no. 7, pp. 2891–2959, 2007.

[15] X. Chen, S. Shen, L. Guo, and S. S. Mao, "Semiconductor-based photocatalytic hydrogen generation," *Chemical Reviews*, vol. 110, no. 11, pp. 6503–6570, 2010.

[16] M. Grätzel, "Materials science: ultrafast colour displays," *Nature*, vol. 414, pp. 575–576, 2001.

[17] H. J. Snaith and L. Schmidt-Mende, "Advances in liquid-electrolyte and solid-state dye-sensitized solar cells," *Advanced Materials*, vol. 19, no. 20, pp. 3187–3200, 2007.

[18] T. Ohsaka, F. Izumi, and Y. Fujiki, "Raman spectrum of anatase, TiO_2," *Journal of Raman Spectroscopy*, vol. 7, no. 6, pp. 321–324, 1978.

[19] G. Liu, H. G. Yang, X. Wang et al., "Enhanced photoactivity of oxygen-deficient anatase TiO_2 sheets with dominant 001 facets," *Journal of Physical Chemistry C*, vol. 113, no. 52, pp. 21784–21788, 2009.

[20] J. Zhang, M. Li, Z. Feng, J. Chen, and C. Li, "UV raman spectroscopic study on TiO_2- I. phase transformation at the surface and in the bulk," *Journal of Physical Chemistry B*, vol. 110, no. 2, pp. 927–935, 2006.

[21] H. G. Yang, C. H. Sun, S. Z. Qiao et al., "Anatase TiO_2 single crystals with a large percentage of reactive facets," *Nature*, vol. 453, no. 7195, pp. 638–641, 2008.

[22] F. Hao, X. Wang, C. Zhou et al., "Efficient ligth harvesting and change collection of dye-sensitized solar cells with (001) faceted single crystalline anatase nanoparticles," *The Journal of Physical Chemistry C*, vol. 116, no. 36, pp. 19164–19172, 2012.

[23] F. Tian, Y. Zhang, J. Zhang, and C. Pan, "Raman spectroscopy: a new approach to measure the percentage of anatase TiO_2 exposed (001) facets," *Journal of Physical Chemistry C*, vol. 116, no. 13, pp. 7515–7519, 2012.

[24] W. Jiao, L. Wang, G. Liu, G. Q. Lu, and H. M. Cheng, "Hollow anatase TiO_2 single crystals and mesocrystals with dominant 101 facets for improved photocatalysis activity and preference," *ACS Catalysis*, vol. 2, pp. 1854–1859, 2012.

[25] Z. Zhao, Z. Li, and Z. Zou, "A Theoretical study of water adsorption and decomposition on the low-index stoichiometric anatase TiO_2 surfaces," *Journal of Physical Chemistry C*, vol. 116, no. 13, pp. 7430–7441, 2012.

[26] J. A. Ibáñez, M. I. Litter, and R. A. Pizarro, "Photocatalytic bactericidal effect of TiO_2 on Enterobacter cloacae. Comparative study with other Gram (−) bacteria," *Journal of Photochemistry and Photobiology A*, vol. 157, no. 1, pp. 81–85, 2003.

[27] M. P. Amézaga, M. R. Silveyra, F. L. Córdoba et al., "TEM evidence ultrastructural alteration on *Pseudomonas aeruginosa* by photocatalytic TiO_2 thin films," *Journal of Photochemistry and Photobiology*, vol. 70, pp. 45–50, 2003.

[28] J. M. C. Robertson, P. K. J. Robertson, and L. A. Lawton, "A comparison of the effectiveness of TiO_2 photocatalysis and UVA photolysis for the destruction of three pathogenic microorganisms," *Journal of Photochemistry and Photobiology A*, vol. 175, no. 1, pp. 51–56, 2005.

[29] K. Ubonchonlakate, L. Sikong, and F. Saito, "Photocatlytic disinfection of *P. aeruginosa* bacterial Ag-doped TiO_2 film," *Procedia Engineering*, vol. 32, pp. 656–662, 2012.